厚生労働科学研究費補助金（難病・がん等の疾患分野の医療の実用化研究事業
（再生医療関係研究分野））
「iPS 細胞等の安定供給と臨床利用のための基盤整備」

分担研究報告書
「体性幹細胞、iPS 細胞等を用いる臨床研究実施のための基盤技術」

研究分担者	**齋藤 充弘**	**大阪大学 未来細胞医療学共同研究講座**	**特任准教授**
研究分担者	澤 芳樹	大阪大学 心臓血管外科学	教授
研究協力者	宮川 繁	大阪大学 心臓血管外科学	講師

【研究要旨】

大阪大学では重症心筋症患者を対象として、ヒト幹細胞指針に適合した自家骨格筋芽細胞シートの臨床研究を進めている。これまで 20 名以上の対象患者から採取した筋肉に含まれる骨格筋芽細胞を培養した経験から、65 歳以上の患者群で筋肉から単離された初代培養細胞数が低い傾向があり、患者背景が影響している可能性が考えられた。さらに、初代培養細胞数が低いと、継代培養後の骨格筋芽細胞の数や純度が低下していた。以上のことから、骨格筋芽細胞の培養に影響与える患者背景を特定することで、より安定的な培養方法につながる可能性が示唆された。

A. 研究目的

大阪大学医学部附属病院未来医療センターでは、基礎研究の早期実用化を目指したトランスレーショナルリサーチ実践の場として,2003 年に医学部附属病院の中央診療施設 の一部門として開設され,ヒト幹細胞臨床研究や遺伝子治 療臨床研究について,審査評価委員会への申請や臨床研究 の実施に必要な書類作成から臨床研究終了までの総合的な サポートを行っている。さらに 6 ユニットの細胞培養調製施設を保有し、国内最多の承認件数を誇るヒト幹細胞臨床研究は国内随一の実施経験で多彩な幹細胞臨床研究の支援を提供できることに加え、GMP 対応施設として治験での利用も可能である。さらに、将来予定されている iPS 細胞由来細胞加工製品の製造を見据えて、細胞調整ユニットの増設を行うとともに、製造支援体制の強化を行った。

研究分担者らが進めているヒト幹細胞指針に適合した自家骨格筋芽細胞シートの臨床研究において、対象患者から採取した筋肉に含まれる骨格筋芽細胞を培養した際に、回収細胞数が少ないことや細胞純度が低下したことが原因で、筋肉の再採取及び骨格筋芽細胞の再培養をするケースがあった。これらにはドナーである患者背景が起因している可能性が考えられた。そこで、今回は臨床研究における細胞培養実績から患者背景が骨格筋芽細胞の培養にどのような影響を与えるかを評価した。

B. 研究方法

回収細胞数・細胞生存率や骨格筋芽細胞の特異的なマーカーである CD56 陽性率（純度）を測定し、移植細胞の品質管理を行っ

た。その結果を元に、患者の年齢・体格・心疾患（拡張型心筋症または虚血性心筋症）でグループ分けして倍加時間・回収細胞数・純度を比較した。

（倫理面への配慮）

本研究においては関連指針等を遵守し、大阪大学倫理委員会の承認を経て慎重に研究を進める。常に人権を尊重した研究を実行し、患者の不利益とならないよう最大限の配慮を行うこととする。

C. 研究結果

65 歳以上の患者群で筋肉から単離された初代培養細胞数が低い傾向があり、患者背景が影響している可能性が考えられた。さらに、初代培養細胞数が低いと、継代培養後の骨格筋芽細胞の数や純度が低下していた。さらに、特定の薬剤の投薬歴が筋肉内の筋芽細胞数に影響を与えている可能性が示唆された。

D. 考按

骨格筋芽細胞の培養に影響与える患者背景や因子について、これまで実施した臨床研究の培養データから推察されできる可能性が示唆されたので、今後も引き続き蓄積される培養データを精査していく必要がある。

E. 結論

自家細胞移植による再生医療等製品の最大の問題点は、培養プロセスを安定化させることである。患者の病歴、投薬歴、疾患の状態によって変わりうる培養プロセスを精査し、変動因子を明らかにするために、引き続き臨床研究のデータの蓄積をすすめる。

F. 健康危険情報

なし

G. 研究発表

1. 論文発表

Cell-sheet Therapy With Omentopexy Promotes Arteriogenesis and Improves Coronary Circulation Physiology in Failing Heart. Kainuma S, Miyagawa S, Fukushima S, Pearson J, Chen YC, Saito A, Harada A, Shiozaki M, Iseoka H, Watabe T, Watabe H, Horitsugi G, Ishibashi M, Ikeda H, Tsuchimochi H, Sonobe T, Fujii Y, Naito H, Umetani K, Shimizu T, Okano T, Kobayashi E, Daimon T, Ueno T, Kuratani T, Toda K, Takakura N, Hatazawa J, Shirai M, Sawa Y. Mol Ther. 2015 Feb;23(2):374-86.

2. 学会発表

なし

H. 知的所有権の取得状況

1. 特許取得

なし

2. 実用新案特許

なし

3. その他

なし

厚生労働科学研究費補助金（難病・がん等の疾患分野の医療の実用化研究事業
（再生医療関係研究分野））
「iPS 細胞等の安定供給と臨床利用のための基盤整備」

分担研究報告書
「幹細胞等の確実な保管および機能解析を実現するための基盤整備」

研究分担者　高島 成二　大阪大学 医化学教室　教授

【研究要旨】
本研究においてはヒト幹細胞の臨床応用に向けた細胞保存設備の整備および、保存される、あるいは保存されている細胞が適切に維持され、安全に再生医療に応用できる施設および細胞解析基盤を構築することを目的とする。本研究分担者は、実際の保存施設の設計および細胞機能評価のためのゲノム・タンパク質解析の基盤構築を行った。本研究においては「ヒト幹細胞を用いる臨床研究に関する指針」ほか関連指針等を遵守し、各施設の倫理委員会の承認を経て慎重に研究を進めた。常に人権を尊重した研究を実行し、患者の不利益とならないよう最大限の配慮を行った。

A. 研究目的

ヒト幹細胞等の適切な保管は、再生医療等の実現に最も必要な事業の一つである。これらの細胞を受け入れ、細胞ストックとして適切な管理を行うためには、保存細胞の性格を正確に把握する必要がある。そのためには微生物感染の有無以外にも、予測しない遺伝子変異による細胞動態の変化や、タンパク質発現変化の動態解析を初期にあるいは定期的に行っていくことが非常に重要である。分担者はこれらが適切に行われるための細胞保存施設の環境整備と、細胞からの遺伝子情報・タンパク質情報の解析基盤の構築を行うことを目的として本事業に参画した。

B. 研究方法

1. 体性幹細胞ならびに iPS 細胞等の細胞凍結保存装置細胞ストックルームの整備

体性幹細胞ならびに iPS 細胞等貯蔵をおこなうために、平成２４年度に当機関内に電子錠を備えた専用のストックルームの設置、コンピュータと連動した自動入出庫管理システムを実現する細胞凍結保管庫（クライオライブラリ）の設置および、既存の液体窒素タンクとの配管整備をおこなった。分担者はこの設計に携わり、特にクリーンでセキュリティの高い保存環境を整える設計に従事した。

2. ヒト幹細胞等の遺伝子・タンパク質解析技術の確立

さまざまな種類の細胞等から、効率よく遺伝子・タンパク質を抽出し、超高速シークエンサーや質量分析等を駆使した解析を行い、幹細胞等の迅速で・的確な機能評価を行う系を確立する。また種々の細胞機能解析し手法も用いて幹細胞等の機能評価も合わせて実行した。

（倫理面への配慮）

本研究においては関連指針等を遵守し、大

阪大学倫理委員会の承認を経て慎重に研究を進める。常に人権を尊重した研究を実行し、患者の不利益とならないよう最大限の配慮を行うこととする。

C. 研究結果

分担者が設計した図面に基づき前室を含めた細胞貯蔵室が完成しH25年11月より液体窒素の充填を開始し、運用を開始した。H26年は実働を開始している。さらに高速シークエンサーを含めた細胞解析環境を整え、Exome解析の解析パイプラインを完成し、すでに１００例以上の解析実績を上げた。

D. 考按

幹細胞等はウイルスを含めた遺伝子操作も行われていることが多く単にその保存を行うだけでなく、一つ一つの細胞においてその機能を含めた遺伝子・タンパク質等の発現が常に一定の形質を保っているか正確にモニターしていかなければならない。そのためには保管施設と併設された細胞解析施設においてこれらの解析が的確行われる環境を作ることの重要性がますます増加すると思われる。幹細胞の機能維持のための細胞機能解析としてどのような系が最も適しているかを今後も追及していくことが再生医療の安全な実現には必須と思われる。今後はさらに遺伝子・タンパク質解析施設を充実させ、iPS細胞等の品質コントロール系を確立させていく必要がある。

E. 結論

クリーンで安全性の高い細胞輸送システムとクライオライブラリによる保管システムの確立と保存細胞の解析基盤の構築をおこなった。

F. 健康危険情報

なし

G. 研究発表

1. 論文発表

なし

2. 学会発表

なし

H. 知的所有権の取得状況

1. 特許取得

なし

2. 実用新案特許

なし

3. その他

なし

厚生労働科学研究費補助金（難病・がん等の疾患分野の医療の実用化研究事業
（再生医療関係研究分野））
「iPS 細胞等の安定供給と臨床利用のための基盤整備」

分担研究報告書
「体性幹細胞付帯情報の収集・管理システムの構築」

研究分担者	新谷 歩	大阪大学 臨床統計疫学寄附講座	教授
研究協力者	山田 知美	大阪大学 臨床統計疫学寄附講座	准教授
研究協力者	山本 紘司	大阪大学 臨床統計疫学寄附講座	准教授
研究協力者	関 季子	大阪大学 医学部附属病院 未来医療開発部	特任研究員

【研究要旨】

iPS 細胞等の保存および機能解析設備のさらなる整備、維持、管理を進め、体性幹細胞ならびに iPS 細胞等の臨床利用の促進を図る本事業においては、幹細胞付帯情報を適切な方法で収集し、統計解析できる状態で管理することが重要となる。本研究の目的は、幹細胞に付帯する情報（培養情報、移植患者関連情報、手術関連情報など個人情報を省いたもの）を体系的に収集・管理するシステムの構築を行うことである。データは REDCap を用いて収集し、大阪大学内の臨床研究専用のサーバーにて管理する。

A. 研究目的

本研究の目的は、幹細胞に付帯する情報（培養情報、移植患者関連情報、手術関連情報など個人情報を省いたもの）を体系的に収集・管理するシステムの構築を行うことである。

B. 研究方法

データは REDCap を用いて収集し、大阪大学内の臨床研究専用のサーバーにて管理する。REDCap システムはインターネットを介して利用するため、サイバー攻撃の対象となる可能性がある。対応策として、アプリケーションレベルでの統合型サーバセキュリティ対策システムを導入する。並行して、今年度は大阪大学眼科領域のデータを対象に REDCap の入力画面を作成する。疾患分類コードの取り込みや、画像添付などの機能追加も行う。

（倫理面への配慮）

本研究においては関連指針等を遵守し、大阪大学倫理委員会の承認を経て慎重に研究を進める。常に人権を尊重した研究を実行し、患者の不利益とならないよう最大限の配慮を行うこととする。

C. 研究結果

アプリケーションレベルでの統合型サーバセキュリティ対策システムの導入により、システムが取扱う情報の不正流出やデータの改竄などのリスクが軽減され、安定したシステム運用と臨床研究データの安全性を保つ基盤を整備した。また、眼科領域の 20 項目について入力画面を作成した。

D. 考按

今年度の予定は概ね順調であった。セキュリティを担保した環境の整備と、眼科領域における REDCap 入力画面を作成したが、実際の運用においては様々な問題が発生することが予想される。運用開始前に SOP の作成と十分なシステムテストを行い、運用開始後は、発生する問題に対処しながら、データの品質を確保するための効率的な運用のノウハウを蓄積する。

E. 結論

セキュリティ対策システムを導入し、安定したシステム運用と臨床研究データの安全性を保つ基盤を整備した。

F. 健康危険情報

なし

G. 研究発表

1. 論文発表

なし

2. 学会発表

なし

H. 知的所有権の取得状況

1. 特許取得

なし

2. 実用新案特許

なし

3. その他

なし

［Ⅳ］

研究成果の刊行に関する一覧表

論文・書籍一覧

英文論文

1. Kawamura T, Miyagawa S, Fukushima S, Yoshida A, Kashiyama N, Kawamura A, Ito E, Saito A, Maeda A, Eguchi H, Toda K, Lee JK, Miyagawa S, Sawa Y. N-glycans: phenotypic homology and structural differences between myocardial cells and induced pluripotent stem cell-derived cardiomyocytes. PLoS One 2014;9(10):e111064.
2. Morimoto T, Kaito T, Kashii M, Matsuo Y, Sugiura T, Iwasaki M, Yoshikawa H. Effect of Intermittent Administration of Teriparatide (Parathyroid Hormone 1-34) on Bone Morphogenetic Protein-Induced Bone Formation in a Rat Model of Spinal Fusion. J Bone Joint Surg Am 2014;96(13):e107.
3. Kaneshiro S, Ebina K, Shi K, Higuchi C, Hirao M, Okamoto M, Koizumi K, Morimoto T, Yoshikawa H, Hashimoto J. IL-6 negatively regulates osteoblast differentiation through the SHP2/MEK2 and SHP2/Akt2 pathways in vitro. J Bone Miner Metab 2014;32(4):378-392.
4. Minegishi Y, Sakai Y, Yahara Y, Akiyama H, Yoshikawa H, Hosokawa K, Tsumaki N. Cyp26b1 within the growth plate regulates bone growth in juvenile mice. Biochem Biophys Res Commun 2014;454(1):12-18.
5. Sugiura T, Kashii M, Matsuo Y, Morimoto T, Honda H, Kaito T, Iwasaki M, Yoshikawa H. Intermittent administration of teriparatide enhances graft bone healing and accelerates spinal fusion in rats with glucocorticoid-induced osteoporosis. Spine J 2015;15(2):298-306.
6. Yoshioka Y, Kosaka N, Konishi Y, Ohta H, Okamoto H, Sonoda H, Nonaka R, Yamamoto H, Ishii H, Mori M, Furuta K, Nakajima T, Hayashi H, Sugisaki H, Higashimoto H, Kato T, Takeshita F, Ochiya T. Ultra-sensitive liquid biopsy of circulating extracellular vesicles using ExoScreen. Nat Commun 2014;5:3591.
7. Fukusumi T, Ishii H, Konno M, Yasui T, Nakahara S, Takenaka Y, Yamamoto Y, Nishikawa S, Kano Y, Ogawa H, Hasegawa S, Hamabe A, Haraguchi N, Doki Y, Mori M, Inohara H. CD10 as a novel marker of therapeutic resistance and cancer stem cells in head and neck squamous cell carcinoma. Br J Cancer 2014;111(3):506-514.
8. Hasegawa S, Eguchi H, Nagano H, Konno M, Tomimaru Y, Wada H, Hama N, Kawamoto K, Kobayashi S, Nishida N, Koseki J, Nishimura T, Gotoh N, Ohno

S, Yabuta N, Nojima H, Mori M, Doki Y, Ishii H. MicroRNA-1246 expression associated with CCNG2-mediated chemoresistance and stemness in pancreatic cancer. Br J Cancer 2014;111(8):1572-1580.

9. Hamabe A, Konno M, Tanuma N, Shima H, Tsunekuni K, Kawamoto K, Nishida N, Koseki J, Mimori K, Gotoh N, Yamamoto H, Doki Y, Mori M, Ishii H. Role of pyruvate kinase M2 in transcriptional regulation leading to epithelial-mesenchymal transition. Proc Natl Acad Sci U S A 2014;111(43):15526-15531.
10. Hamabe A, Yamamoto H, Konno M, Uemura M, Nishimura J, Hata T, Takemasa I, Mizushima T, Nishida N, Kawamoto K, Koseki J, Doki Y, Mori M, Ishii H. Combined evaluation of hexokinase 2 and phosphorylated pyruvate dehydrogenase-E1alpha in invasive front lesions of colorectal tumors predicts cancer metabolism and patient prognosis. Cancer Sci 2014;105(9):1100-1108.
11. Takeyari S, Yamamoto T, Kinoshita Y, Fukumoto S, Glorieux FH, Michigami T, Hasegawa K, Kitaoka T, Kubota T, Imanishi Y, Shimotsuji T, Ozono K. Hypophosphatemic osteomalacia and bone sclerosis caused by a novel homozygous mutation of the FAM20C gene in an elderly man with a mild variant of Raine syndrome. Bone 2014;67:56-62.
12. Kubota T, Kitaoka T, Miura K, Fujiwara M, Ohata Y, Miyoshi Y, Yamamoto K, Takeyari S, Yamamoto T, Namba N, Ozono K. Serum fibroblast growth factor 23 is a useful marker to distinguish vitamin D-deficient rickets from hypophosphatemic rickets. Horm Res Paediatr 2014;81(4):251-257.
13. Kitaoka T, Miyoshi Y, Namba N, Miura K, Kubota T, Ohata Y, Fujiwara M, Takagi M, Hasegawa T, Juppner H, Ozono K. Two Japanese familial cases of Caffey disease with and without the common COL1A1 mutation and normal bone density, and review of the literature. Eur J Pediatr 2014;173(6):799-804.
14. Iwatsuki K, Yoshimine T. Regenerative Medicine for Spinal Cord Injury Using Olfactory Mucosa Autografts. In: Sankai Y, Suzuki K, Hasegawa Y (eds), *Cybernics*: Springer Japan; 2014:99-108.
15. Iwatsuki K, Yoshimine T, Sankai Y, Tajima F, Umegaki M, Ohnishi Y-I, Ishihara M, Ninomiya K, Moriwaki T. Involuntary muscle spasm expressed as motor evoked potential after olfactory mucosa autograft in patients with chronic spinal cord injury and complete paraplegia. J Biomedical Science and Engineering 2013;908-916.

16. Iinuma S, Aikawa E, Tamai K, Fujita R, Kikuchi Y, Chino T, Kikuta J, McGrath JA, Uitto J, Ishii M, Iizuka H, Kaneda Y. Transplanted Bone Marrow-Derived Circulating PDGFRalpha+ Cells Restore Type VII Collagen in Recessive Dystrophic Epidermolysis Bullosa Mouse Skin Graft. Journal of immunology 2015;194(4):1996-2003.
17. Fujita R, Tamai K, Aikawa E, Nimura K, Ishino S, Kikuchi Y, Kaneda Y. Endogenous Mesenchymal Stromal Cells in Bone Marrow Are Required to Preserve Muscle Function in mdx Mice. Stem cells 2015;33(3):962-975.
18. Moritsugu R, Tamai K, Nakano H, Aizu T, Nakajima K, Yamazaki T, Sawamura D. Functional analysis of the nuclear localization signal of the POU transcription factor Skn1a in epidermal keratinocytes. Int J Mol Med 2014;34(2):539-544.

和文論文

1. 岩月幸一. 自家嗅粘膜移植による脊髄再生医療. 脳神経外科ジャーナル 2013;22(6):452-458.
2. 岩月幸一, 吉峰俊樹, 大西諭一郎, 二宮貢士, 森脇崇. 嗅粘膜移植による脊髄再生医療. Anesthesia 21 century 2013;15(3-47):44-49.

書籍

1. 北畠康司. 新しいゲノム編集技術（TALENおよびCRISPR/Cas9システム）とその可能性. 再生医療シリーズ「脳神経系の再生医学　－発生と再生の融合的新展開－」 2015;155-160.

［V］

研究成果の別刷

OPEN ACCESS Freely available online

PLOS | ONE

N-Glycans: Phenotypic Homology and Structural Differences between Myocardial Cells and Induced Pluripotent Stem Cell-Derived Cardiomyocytes

Takuji Kawamura[1], Shigeru Miyagawa[1], Satsuki Fukushima[1], Akira Yoshida[2], Noriyuki Kashiyama[1], Ai Kawamura[1], Emiko Ito[1], Atsuhiro Saito[1], Akira Maeda[3], Hiroshi Eguchi[3], Koichi Toda[1], Jong-Kook Lee[2], Shuji Miyagawa[3], Yoshiki Sawa[1]*

1 Department of Cardiovascular Surgery, Osaka University Graduate School of Medicine, Suita, Osaka, Japan, **2** Department of Cardiovascular Regenerative Medicine, Osaka University Graduate School of Medicine, Suita, Osaka, Japan, **3** Division of Organ Transplantation, Department of Surgery, Osaka University Graduate School of Medicine, Suita, Osaka, Japan

Abstract

Cell surface glycans vary widely, depending on cell properties. We hypothesized that glycan expression on induced pluripotent stem cells (iPSCs) might change during cardiomyogenic differentiation toward the myocardial phenotype. *N*-glycans were isolated from iPSCs, iPSC-derived cardiomyocytes (iPSC-CM), and original C57BL/6 mouse myocardium (Heart). Their structures were analyzed by a mapping technique based on HPLC elution times and MALDI-TOF/MS spectra. Sixty-eight different *N*-glycans were isolated; the structures of 60 of these *N*-glycans were identified. The quantity of high-mannose type (immature) *N*-glycans on the iPSCs decreased with cardiomyogenic differentiation, but did not reach the low levels observed in the heart. We observed a similar reduction in neutral *N*-glycans and an increase in fucosylated or sialyl *N*-glycans. Some structural differences were detected between iPSC-CM and Heart. No *N*-glycolyl neuraminic acid (NeuGc) structures were detected in iPSC-CM, whereas the heart contained numerous NeuGc structures, corresponding to the expression of cytidine monophosphate-*N*-acetylneuraminic acid hydroxylase. Furthermore, several glycans containing Galα1-6 Gal, rarely identified in the other cells, were detected in the iPSC-CM. The expression of *N*-glycan on murine iPSCs changed toward the myocardial phenotype during cardiomyogenic differentiation, leaving the structural differences of NeuGc content or Galα1-6 Gal structures. Further studies will be warranted to reveal the meaning of the difference of *N*-glycans between the iPSC-CM and the myocardium.

Citation: Kawamura T, Miyagawa S, Fukushima S, Yoshida A, Kashiyama N, et al. (2014) *N*-Glycans: Phenotypic Homology and Structural Differences between Myocardial Cells and Induced Pluripotent Stem Cell-Derived Cardiomyocytes. PLoS ONE 9(10): e111064. doi:10.1371/journal.pone.0111064

Editor: Toru Hosoda, Tokai University, Japan

Received April 30, 2014; **Accepted** September 19, 2014; **Published** October 30, 2014

Data Availability: The authors confirm that all data underlying the findings are fully available without restriction. All relevant data are within the paper and its Supporting Information files.

Funding: YS received the funding to support this work from the Research Center Network for Realization of Regenerative Medicine managed by Centers for Clinical Application Research on Specific Disease/Organ and funded by Japan Science and Technology Agency. The funders had no role in study design, data collection and analysis, decision to publish, or preparation of the manuscript.

Competing Interests: The authors have declared that no competing interests exist.

* Email: sawa-p@surg1.med.osaka-u.ac.jp

Introduction

In vitro generation of cardiac myocytes by reprogramming is a promising technology in developing cell-transplant therapy for advanced cardiac failure [1] and drug discovery for a variety of cardiac diseases [2]. For both purposes, induced pluripotent stem cells (iPSCs) are most useful, since generation and cardiomyogenic differentiation of iPSCs has been standardized in human and a number of animals [3,4]. In fact, derivatives of iPSCs have been developed to the pre-clinical stage for cell transplantation therapy [5], while cardiac myocytes generated from patient-specific iPSCs have been studied to explore pathologic mechanisms and guide drug discovery [6,7]. However, cardiac myocyte preparations from iPSCs contain immature phenotypes, observed by electrophysiology, electron microscopy, and immunohistochemistry [8,9]; this may limit the safety and efficacy of cell transplantation therapy or reduce the accuracy and efficiency of drug discovery. The maturity of iPSC-derived cardiac myocytes (iPSC-CMs) has not been comprehensively or quantitatively evaluated.

Cell surface glycans have several important functions interacting with numerous proteins, including growth factors, morphogens and adhesion molecules, modulating dynamic cellular mechanisms such as cell-cell adhesion, cell activation, and malignant alterations [10–12]. In early mammalian embryos, associated with fertilization, some *N*-glycans play important roles of cell-cell adhesion [13–15]. In addition, cellular responsiveness to growth or arrest depends on total *N*-glycan number and the degree of branching of cell surface glycoproteins [16]. Furthermore, heparan sulfate, a kind of glycans, is required for embryonic stem cell (ESC) pluripotency, in particular lineage specification into mesoderm through facilitation of FGF and BMP signaling by stabilizing BMP ligand [17], leading the evidence that the expression patterns of cell surface glycans on ESCs changes during differentiation [18]. Thus, we hypothesized that cell surface glycan expression may

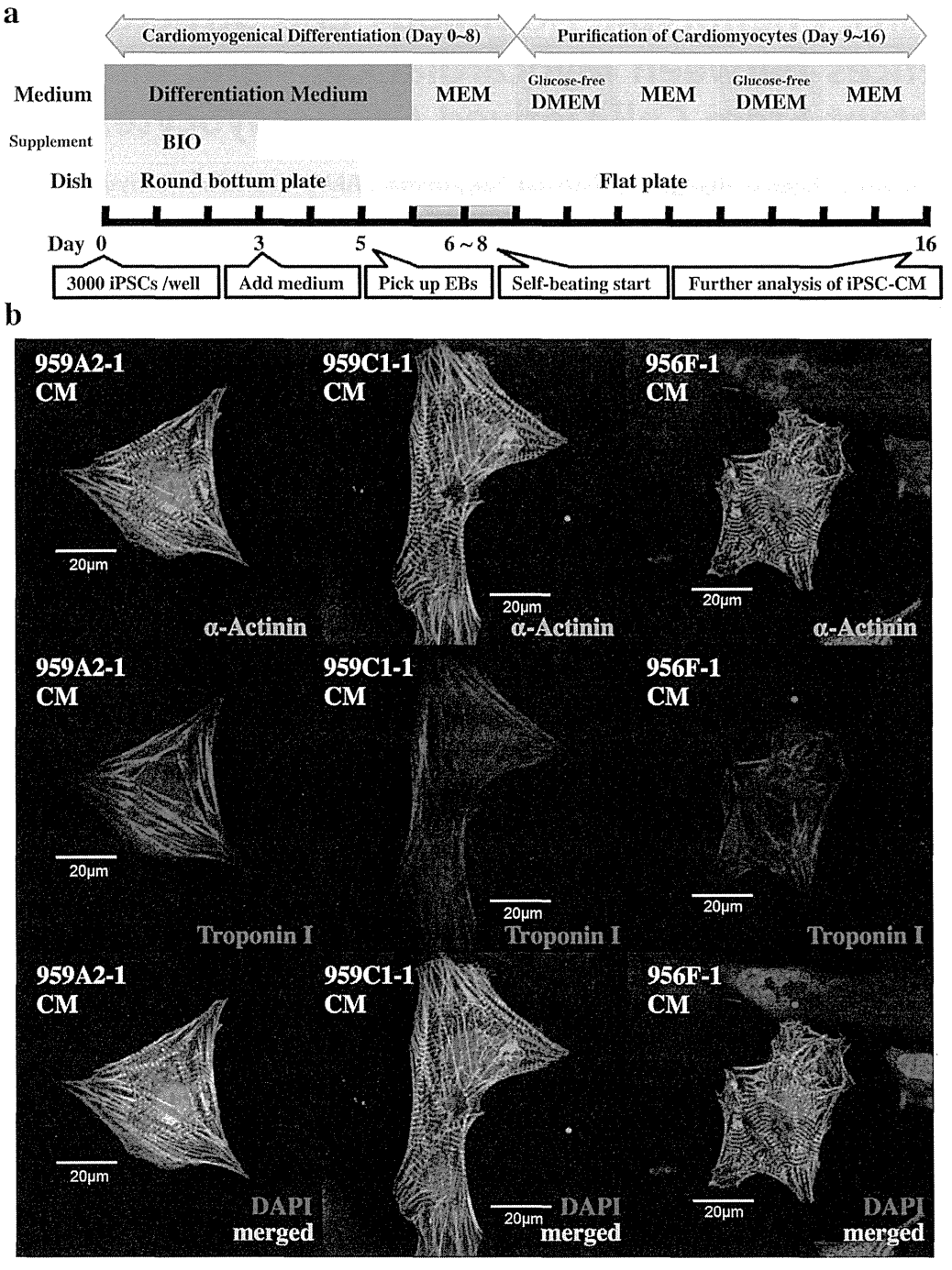

Figure 1. Cardiomyogenic differentiation of iPSCs and cardiomyocyte purification. (a) The cardiomyogenic differentiation protocol and cardiomyocyte purification process are illustrated. (b) IPSC-CMs stained with anti-α-actinin antibody (Alexa Fluor 488), anti-troponin I (Alexa Fluor 594) and DAPI, were analyzed with a confocal laser scanning microscopy. Abbreviations: EB, embryonic body; MEM, Modified Eagle's Medium; DMEM, Dulbecco's Modified Eagle's Medium; BIO, 6-bromoindirubin-3′-oxime.
doi:10.1371/journal.pone.0111064.g001

change during the course of cardiomyogenic differentiation of iPSCs *in vitro*. We analyzed *N*-glycan expression in undifferentiated iPSCs, iPSC-CMs, and adult murine myocardium by HPLC, to identify potential indicators of the maturity of differentiating cardiomyocytes from iPS cells *in vitro*.

Materials and Methods

Animal care procedures were consistent with the "Guide for the Care and Use of Laboratory Animals" (National Institutes of Health publication). Experimental protocols were approved by the

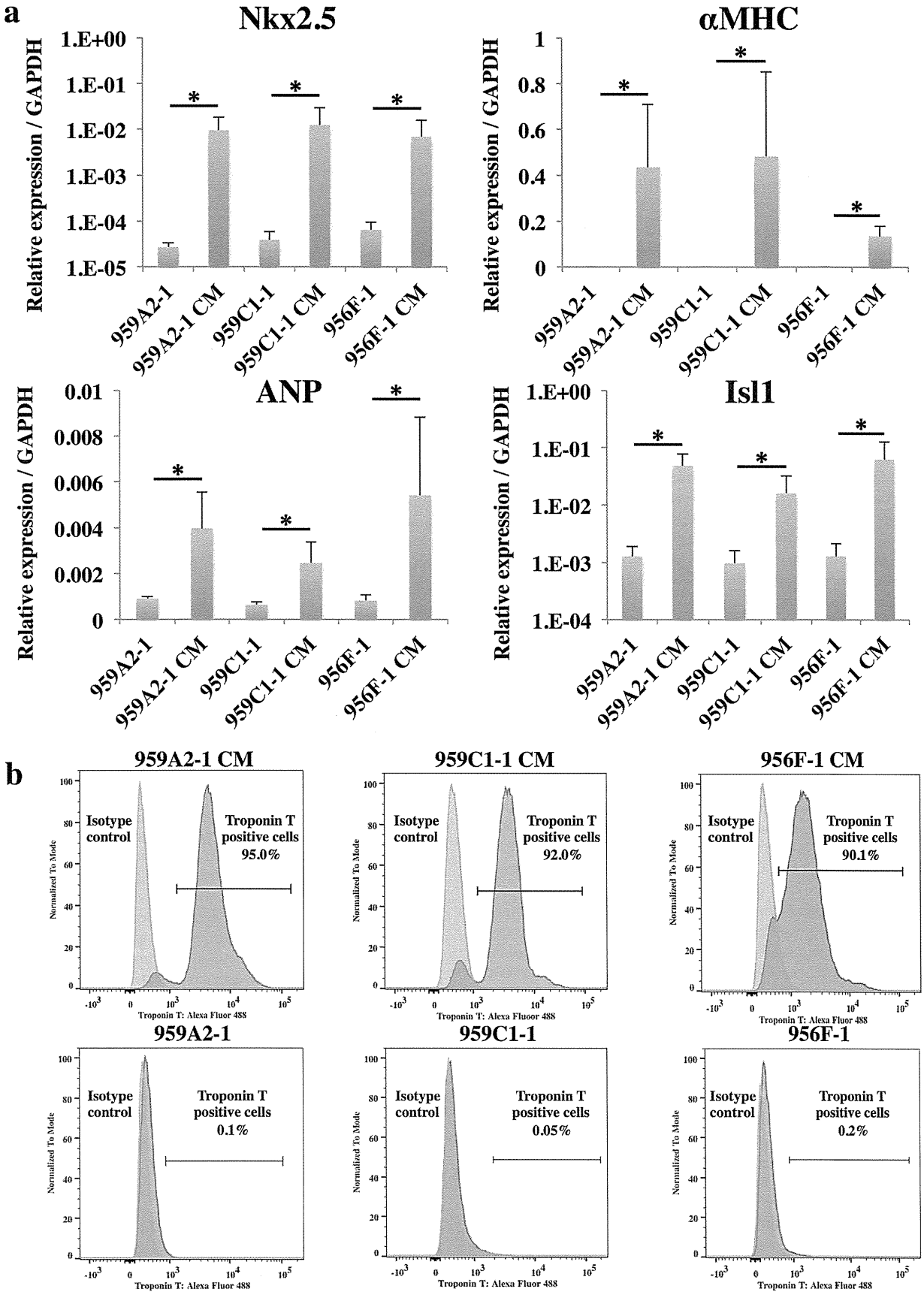
a
Nkx2.5
αMHC
ANP
Isl1
Relative expression / GAPDH
959A2-1
959A2-1 CM
959C1-1
959C1-1 CM
956F-1
956F-1 CM
b
959A2-1 CM
959C1-1 CM
956F-1 CM
959A2-1
959C1-1
956F-1
Isotype control
Troponin T positive cells 95.0%
Troponin T positive cells 92.0%
Troponin T positive cells 90.1%
Troponin T positive cells 0.1%
Troponin T positive cells 0.05%
Troponin T positive cells 0.2%
Normalized To Mode
Troponin T: Alexa Fluor 488

Figure 2. Highly purified iPSC-CMs expressing cardiomyocyte marker genes. (a) Transcript expression of Nkx2.5, αMHC, ANP and Isl1 in the iPSCs and the iPSC-CMs were analyzed by real-time PCR. Results are expressed as the mean ± standard deviation. *P<0.05. (b) IPSC-CMs and iPSCs stained with anti-troponin T antibody or the isotype control, followed by Alexa Fluor 488-conjugated anti-mouse IgG antibody, were analyzed by flow cytometry.
doi:10.1371/journal.pone.0111064.g002

Ethics Review Committee for Animal Experimentation of Osaka University Graduate School of Medicine.

Cardiomyogenic differentiation of murine iPSCs *in vitro*

We used the murine iPSC lines, 959A2-1, 959C1-1, 956F-1 (generous gifts from Dr. Okita and Professor Yamanaka of the Center for iPS Cell Research and Application, Kyoto University, Kyoto, Japan). The cell lines were generated from C57BL/6 (B6) (CLEA) mouse embryonic fibroblasts by introducing *Oct3/4, Sox2, Klf4*, and *c-Myc* without viral vectors as described [19]. The iPSCs were cultured in the absence of serum and feeder cells by using ESGRO Complete PLUS Clonal Grade Medium (Millipore).

Cardiomyogenic differentiation of the iPSCs was performed as described [20,21], with modifications, followed by purification with glucose-free medium supplemented with lactic acid [22]; iPSCs (3×10^3) were resuspended in 100-μL aliquots of differentiation medium [DM; Dulbecco's Modified Eagle's Medium (DMEM; Nacalai Tesque) containing 15% fetal bovine serum (FBS; Biofill), 100 μmol/L non-essential amino acids (NEAA; Invitrogen), 2 mmol/L L-glutamine (Invitrogen), and 0.1 mmol/L 2-mercaptoethanol (Invitrogen)] containing 0.2 μmol/L 6-bromoindirubin-3′-oxime (BIO; a glycogen synthase kinase-3β inhibitor, to activate the Wnt-signaling pathway) (Calbiochem), and cultured in 96-well Corning Costar Ultra-Low attachment multiwell plates (Sigma-Aldrich) for 3 days. On day 3, an additional 100 μL DM without BIO was added to each well. On day 5, individual embryoid bodies (EBs) were transferred to 100-mm gelatin-coated dishes (250 EBs per dish). On days 6, 7, 10, 11, 14, and 15 the medium was exchanged for serum-free Modified Eagle's Medium (MEM; Invitrogen) with insulin transferrin-selenium-X (Invitrogen). On days 8, 9, 12, and 13, the medium was exchanged for Glucose-free DMEM (no glucose, no pyruvate, Invitrogen) supplemented with 4 mmol/L lactic acid (Wako Pure Chemical) for purification of cardiomyocytes. On day 16, the contracting cell clusters were used as cardiomyogenically differentiated iPSCs (959A2-1 CMs, 959C1-1 CMs, 956F-1 CMs: iPSC-CMs). The protocol and purification process are illustrated in Figure 1a.

Adult cardiac tissue from B6 mice (CLEA) was used as a control. Male B6 mice (8 weeks old) were sacrificed by intravenous administration of potassium chloride under inhalation anesthesia of isoflurane, and heart tissue from the left ventricle was harvested for further studies and labeled "Heart".

Immunohistochemistry analysis

IPSC-CMs were dissociated with 0.25% trypsin-EDTA and then fixed with 4% paraformaldehyde. The cells were stained with the following primary antibodies: mouse anti-α-actinin antibody (Sigma-Aldrich) and rabbit anti-troponin I antibody (Abcam), and then visualized by the following secondary antibodies: Alexa Fluor 488 donkey anti-mouse IgG (Invitrogen) and Alexa Fluor 594 goat anti-rabbit IgG (Invitrogen). The nucleus of the cells were stained with 4′, 6-Diamidino-2-phenylindole dihydrochloride (DAPI) and then observed with a confocal laser scanning microscopy FV1200 (Olympus).

Ca^{2+} transient measurement and pharmacological analysis

5 μM Fluo-8 regents (AAT Bioquest, Inc.) in serum-free MEM was added to iPSC-CMs after the cells were washed with phosphate buffered saline. The cells were incubated at 37°C for 30 min and then observed with a fluorescence microscopy. Fluorescence intensity of Fluo-8 dye was sequentially measured using iQ2 software (ANDOR) pre and post the administration of 1 μM isoproterenol.

Flow cytometry

IPSC-CMs were dissociated with 0.25% trypsin-EDTA and then fixed with CytoFix fixation buffer (BD) for 20 min. The cells were permeabilized with Perm/Wash buffer (BD) at room temperature for 10 min and then incubated with mouse anti-troponin T antibody (Thermo) for 30 min. Cells were washed with Perm/Wash buffer prior to incubation with the Alexa Fluor 488 rabbit anti-mouse IgG secondary antibody (Invitrogen) at room temperature for 30 min. These cells were analyzed on a FACS Canto II (BD).

Characterization of *N*-glycans derived from iPSCs, iPSC-CM, and Heart

All experimental procedures, including chromatography conditions and glycosidase treatments, have been described previously [23]. Cultured undifferentiated iPSCs, iPSC-CMs, and the heart tissue were treated with chloroform–methanol, then subjected to proteolysis with chymotrypsin and trypsin, followed by glycoamidase A digestion to release *N*-glycans. After removal of peptides, the reducing ends of the *N*-glycans were derivatized with 2-aminopyridine (Wako). This mixture was applied to a diethylaminoethyl (DEAE) column (Tosoh) or a TSK-gel Amide-80 column (Tosoh); each fraction from the amide column was then applied to a Shim-pack HRC-octadecyl silane (ODS) column (Shimadzu). The elution times of individual peaks from the amide-silica and ODS columns were normalized to a pyridylamino (PA)-derivatized isomalto-oligosaccharide with a known degree of polymerization, and are represented as glucose units (GU). Thus, each compound from these two columns provided a unique set of GU values, which corresponded to the coordinates of the 2D HPLC map. The PA-oligosaccharides were identified by comparison to the coordinates of ~500 reference PA-oligosaccharides in a homemade web application, GALAXY (http://www.glycoanalysis.info/galaxy2/ENG/index.jsp) [24]. The calculated HPLC map based on the unit contribution values was used to estimate some high-mannose type PA-oligosaccharides. The PA-oligosaccharides were co-chromatographed with the reference to PA-oligosaccharides on the columns to confirm their identities. PA-glycans that did not correspond to any of the *N*-glycans registered in GALAXY were trimmed by exoglycosidase to produce a series of known glycans [25].

Mass spectrometry

PA-oligosaccharides were analyzed by matrix-assisted laser desorption/ionization time-of-flight mass spectrometric (MALDI-TOF/MS). The matrix solution was prepared as follows: 10 mg of 2,5-Dihydroxybenzoic acid (Sigma) was dissolved in 1:1 (v/v)

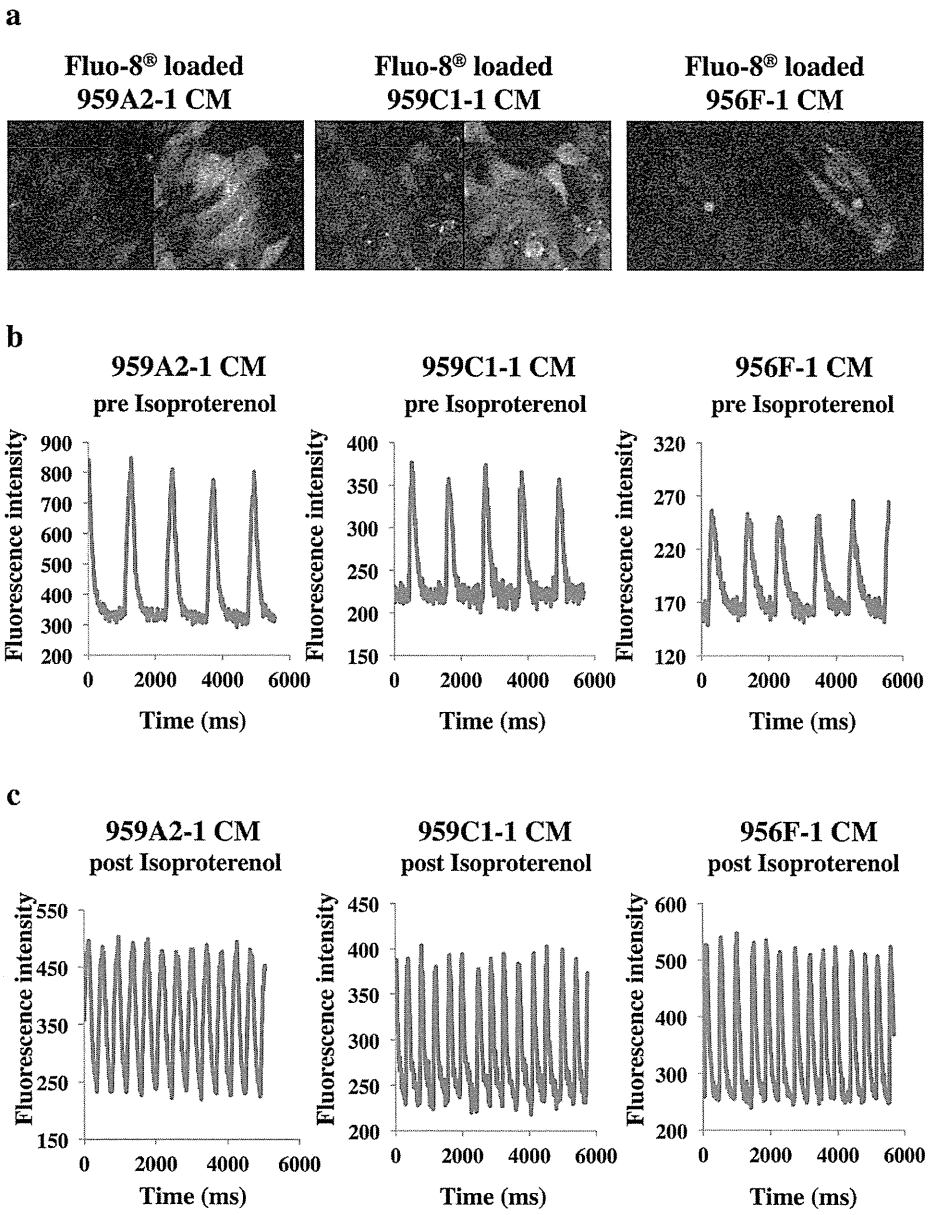

Figure 3. Ca^{2+} transient measurement of iPSC-CMs pre and post the administration of isoproterenol. (a) Fluo-8 loaded iPSC-CMs at the time of low (left) and high (right) fluorescence. (b), (c) Sequentially measured fluorescence intensity of Fluo-8 loaded iPSC-CMs pre (b) and post (c) the administration of 1 μM isoproterenol.
doi:10.1371/journal.pone.0111064.g003

acetonitrile/water (1 mL). Stock solutions of PA-glycans were prepared by dissolving them in pure water. One microliter of a sample solution was mixed on the target spot of a plate with 1 μL matrix solution and then allowed to air-dry. MALDI-TOF/MS data were acquired in the positive mode on an AXIMA-CFR (Shimadzu) operated in linear mode.

Materials

Glycoamidase A from sweet almond, α-mannosidase, β-galactosidase, and β-*N*-acetylhexosaminidase from jack bean were purchased from Seikagaku Kogyo (Tokyo, Japan). α-Galactosidase from coffee bean was purchased from Oxford GlycoSciences (Oxford, UK). Trypsin and chymotrypsin were obtained from Sigma (St. Louis, MO). Pronase protease from *Streptomyces griseus* was from Calbiochem (San Diego, CA). The pyridylamino (PA) derivatives of isomalto-oligosaccharides 4–20 (indicating the degree of polymerization of glucose residues) and reference PA-oligosaccharides were purchased from Seikagaku Kogyo.

Semi-quantitative PCR

DNA-free total RNA was extracted with the RNeasy RNA isolation Kit (Qiagen) and reverse-transcribed into cDNA using Omniscript reverse transcriptase (Qiagen), then analyzed by quantitative real-time PCR on an ABI PRISM 7700 thermocycler (Applied Biosystems) with the following TaqMan gene expression assays (Applied Biosystems): ST3Gal-III (Gal β1-3(4) GlcNAc α-2,

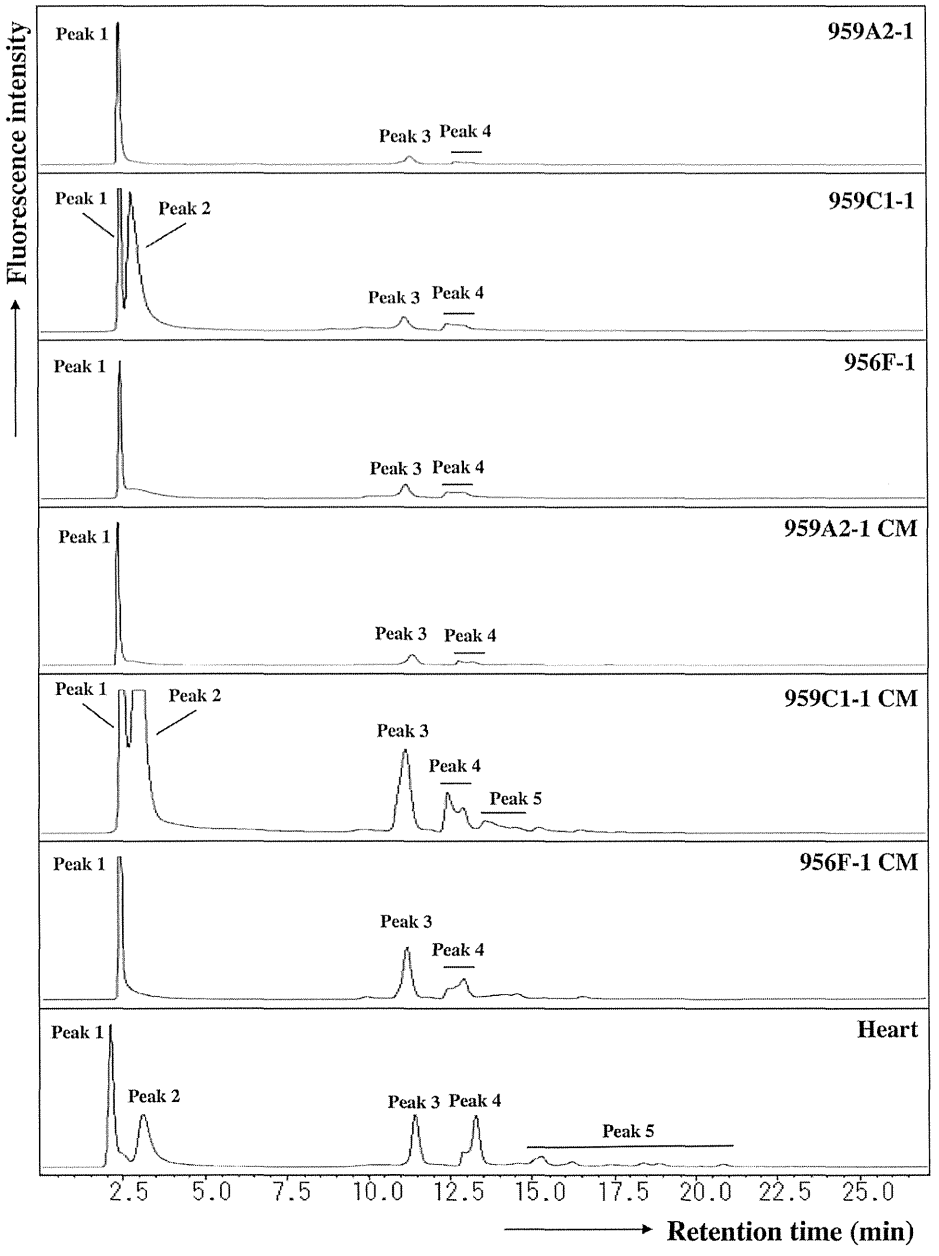

Figure 4. Anion-exchange DEAE elution profiles of PA-glycans. PA-glycans were fractionated according to their sialic acid content as neutral (peak 1), monosialyl (peak 3), and disialyl (peak 4) oligosaccharide fractions. Peaks 2 and 5 represent fractions containing no detectable PA-oligosaccharides.
doi:10.1371/journal.pone.0111064.g004

3-sialyltransferase), Mm00493353_m1; ST4Gal-IV (Gal β1-4(3) GlcNAc α-2, 3-sialyltransferase), Mm00501503_m1; ST6Gal-I (Gal β1-4 GlcNAc α-2, 6-sialyltransferase), Mm00486119_m1; CMAH (cytidine monophosphate-*N*-acetylneuraminic acid hydroxylase), Mm00483341_m1; GAPDH (glyceraldehyde-3-phosphate dehydrogenase), and Mm03302249_g1 and with SYBR Green dye (Applied Biosystems) using the following primers: Nkx2.5 F, 5′- CAAGTGCTCTCCTGCTTTCC -3′ R, 5′- GGCTTTGTCCAGCTCCACT -3′; αMHC (α-myosin heavy chain) F, 5′- GAGATTTCTCCAACCCAG -3′ R, 5′- TCTGACTTTCGGAGGTACT-3′; ANP (atrial natriuretic peptide) F, 5′-AAAGAAACCAGAGTGGGCAGAG -3′ R, 5′- CCAGGGTGATGGAGAAGGAG -3′; Isl1 F, 5′- TTTCCCTGTGTGTTGGTTGC -3′ R, 5′- TGATTACACTCCGCACATTTCA -3′; GAPDH F, 5′- CCAGTATGACTCCACTCACG -3′ R, 5′- GACTCCACGACATACTCAGC -3′. All experiments were performed by the relative standard curve method in three independent, triplicate experiments. Statistical comparison of the data was performed by Student's t-test.

Results

Highly purified cardiomyocytes derived from iPSCs

Cardiomyogenic differentiation was induced in murine iPSCs by using a slightly modified culture protocol (Figure 1a). The iPSC-CMs showed significantly higher expressions of Nkx2.5,

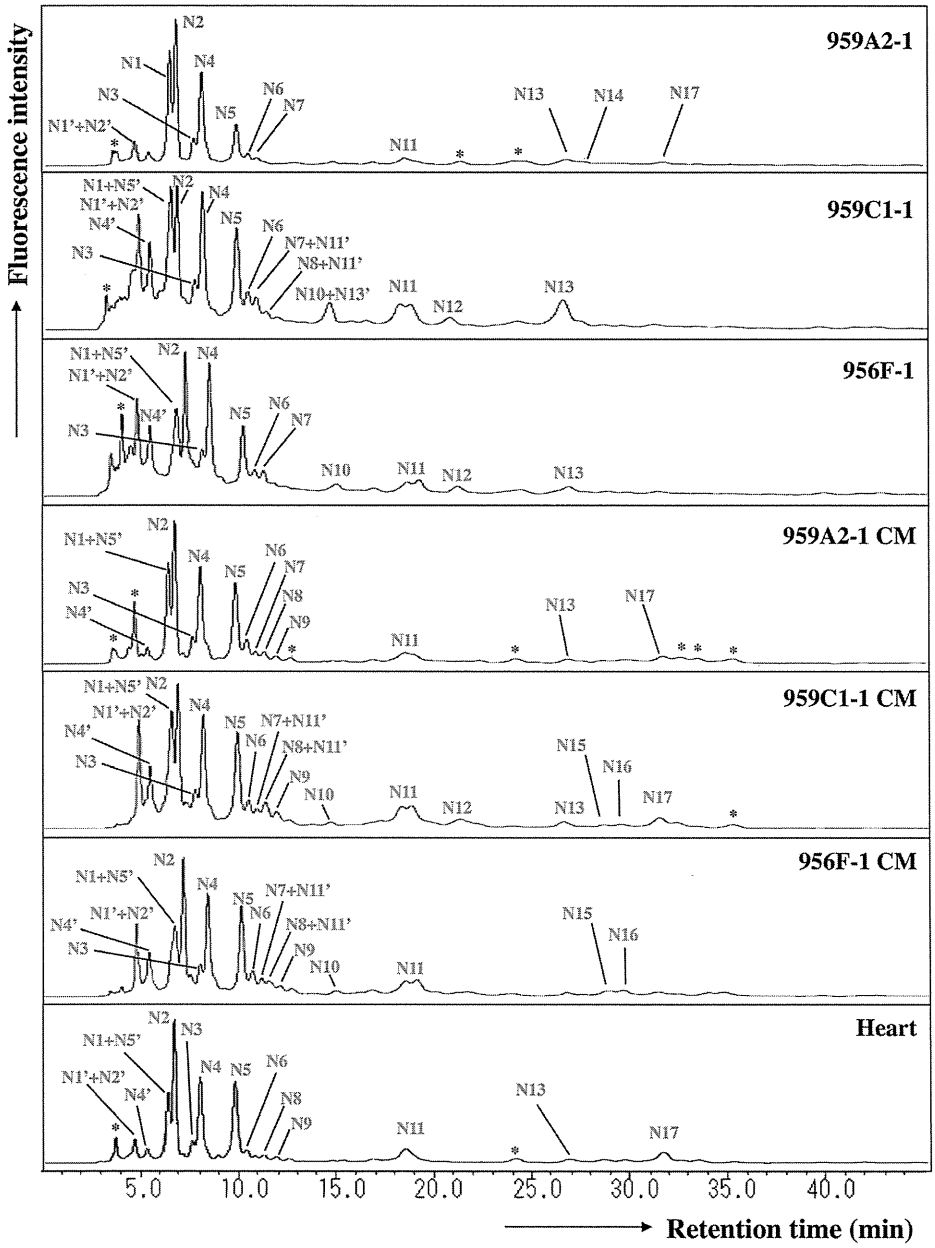

Figure 5. Reverse-phase ODS elution profiles of the neutral PA-glycans. The neutral fractions were individually applied to the ODS column and eluted according to their hydrophobicity. N1′, N2′, N4′, N5′ and N11′: epimerization of N1, N2, N4, N5 and N11. *Fractions containing no detectable PA-oligosaccharides.
doi:10.1371/journal.pone.0111064.g005

αMHC, ANP and Isl1 than undifferentiated iPSCs by semi-quantitative real-time PCR (Figure 2a), and showed sarcomere structures observed by immunohistological staining of α-actinin and troponin I (Figure 1b). The iPSC-CMs were functional with Ca^{2+} transient measurement (Figure 3a, b) and their beating rates were increased by the administration of isoproterenol (Figure 3c), meaning they had β-adrenergic receptors. Nearly all of the iPSC-CMs exhibited spontaneous and regular beating at room temperature (Video S1). The differentiation efficiency of murine iPSC was evaluated by flow cytometry analysis. More than 95% of the 959A2-1 CMs, 92% of the 959C1-1 CMs and 90% of the 956F-1 CMs were positive for troponin T (Figure 2b), while the undifferentiated iPSCs rarely expressed troponin T (Figure 2b).

N-Glycans isolated from iPSCs, iPSC-CM, and Heart

N-glycans extracted from undifferentiated iPSCs (959A2-1: 26 mg, 959C1-1: 11 mg and 956F-1: 10 mg of protein), iPSC-CM (959A2-1 CM: 15 mg, 959C1-1 CM: 12 mg and 956F-1 CM: 5.5 mg of protein), and the B6 heart muscle (82 mg of protein) were separated on a diethylaminoethyl (DEAE) column into five peaks, based on increasing acidity. Peak 1 represented a neutral (N) fraction, peak 3 a monosialyl (M) fraction, and peak 4 a disialyl

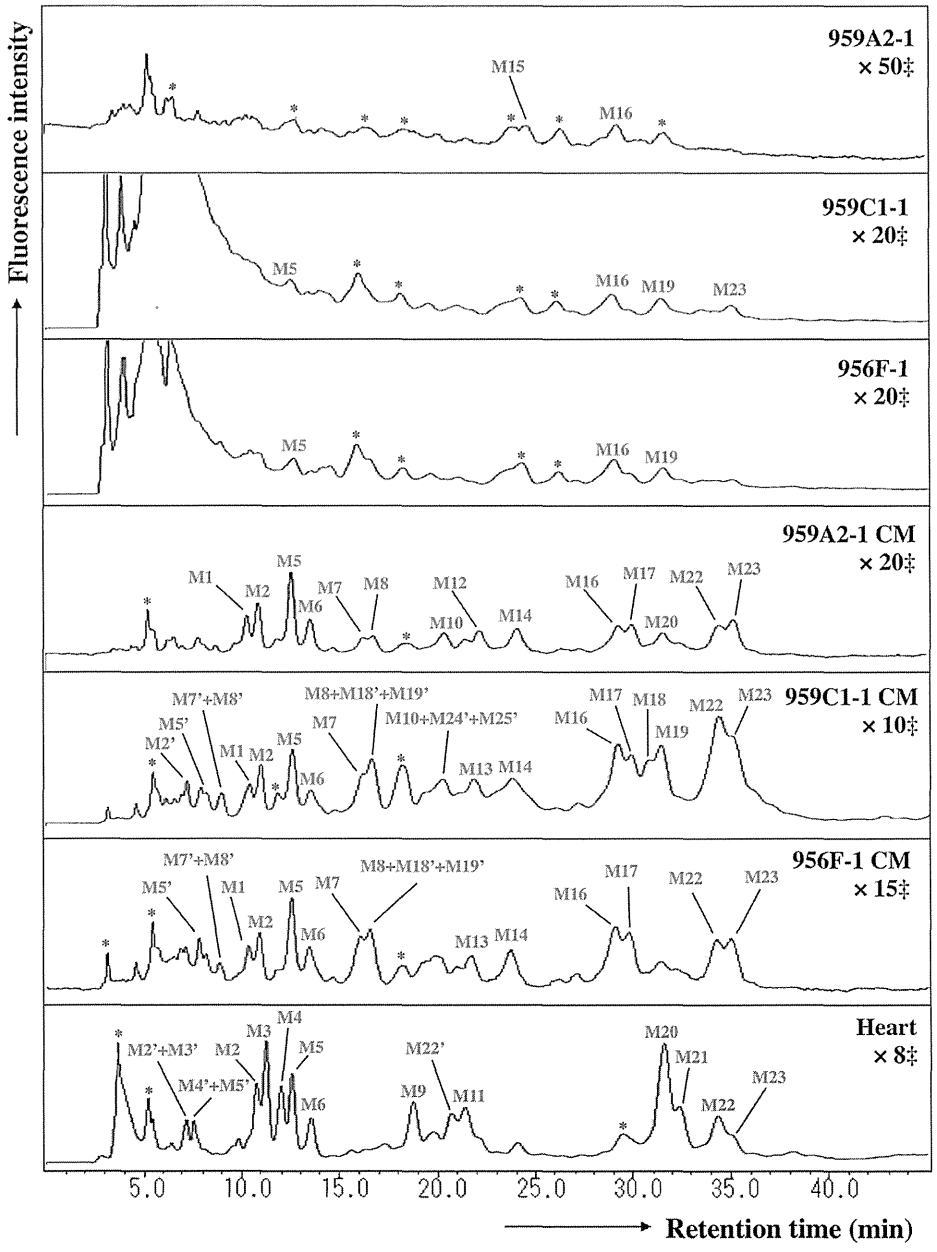

Figure 6. Reverse-phase ODS elution profiles of monosialyl PA-glycans. The monosialyl fractions were individually applied to the ODS column and eluted according to their hydrophobicity. M2′, M3′, M4′, M5′, M7′, M8′, M18′, M19′, M22′, M24′ and M25′: epimerization of M2, M3, M4, M5, M7, M8, M18, M19, M22, M24 and M25. *Fractions containing no detectable PA-oligosaccharides. ‡Magnification ratio to the fluorescence intensity of asialoglycan of each sample.
doi:10.1371/journal.pone.0111064.g006

(D) fraction. Glycan fractions in each of these peaks were as follows: iPSCs yielded 97% N, 0.5% M, 2.6% D (959A2-1), 98% N, 0.7% M, 1.1% D (959C1-1) and 96% N, 1.1% M, 3.1% D (956F-1) peak areas, iPSC-CMs yielded 89% N, 6.4% M, 4.4% D (959A2-1 CM), 79% N, 16% M, 4.8% D (959C1-1 CM) and 82% N, 10% M, 7.9% D (956F-1 CM) and Heart yielded 55% N, 19% M, and 25% D (Figure 4).

The ODS column separated the neutral fraction (Peak 1) into fractions N1–N17 (Figure 5), the monosialyl fraction (Peak 3) into fractions M1–M23 (Figure 6), and the disialyl fraction (Peak 4) into fractions D1–D12 (Figure 7). The signatures of each fraction differed between groups. These ODS fractions were individually fractionated on an amide column and analyzed by MALDI-TOF/MS. The N2, M6, M11, M14, M20, D4, D5, and D10 fractions contained two types of *N*-glycans, and the N6, N9, N11 and M2 fractions three types (data not shown). Thus, 68 different *N*-glycans were isolated from iPSCs, iPSC-CMs, and Heart.

Structures of *N*-Glycans isolated from iPSCs, iPSC-CM, and Heart

The isolated *N*-glycans were analyzed by means of a mapping technique based on their HPLC elution positions and MALDI-TOF/

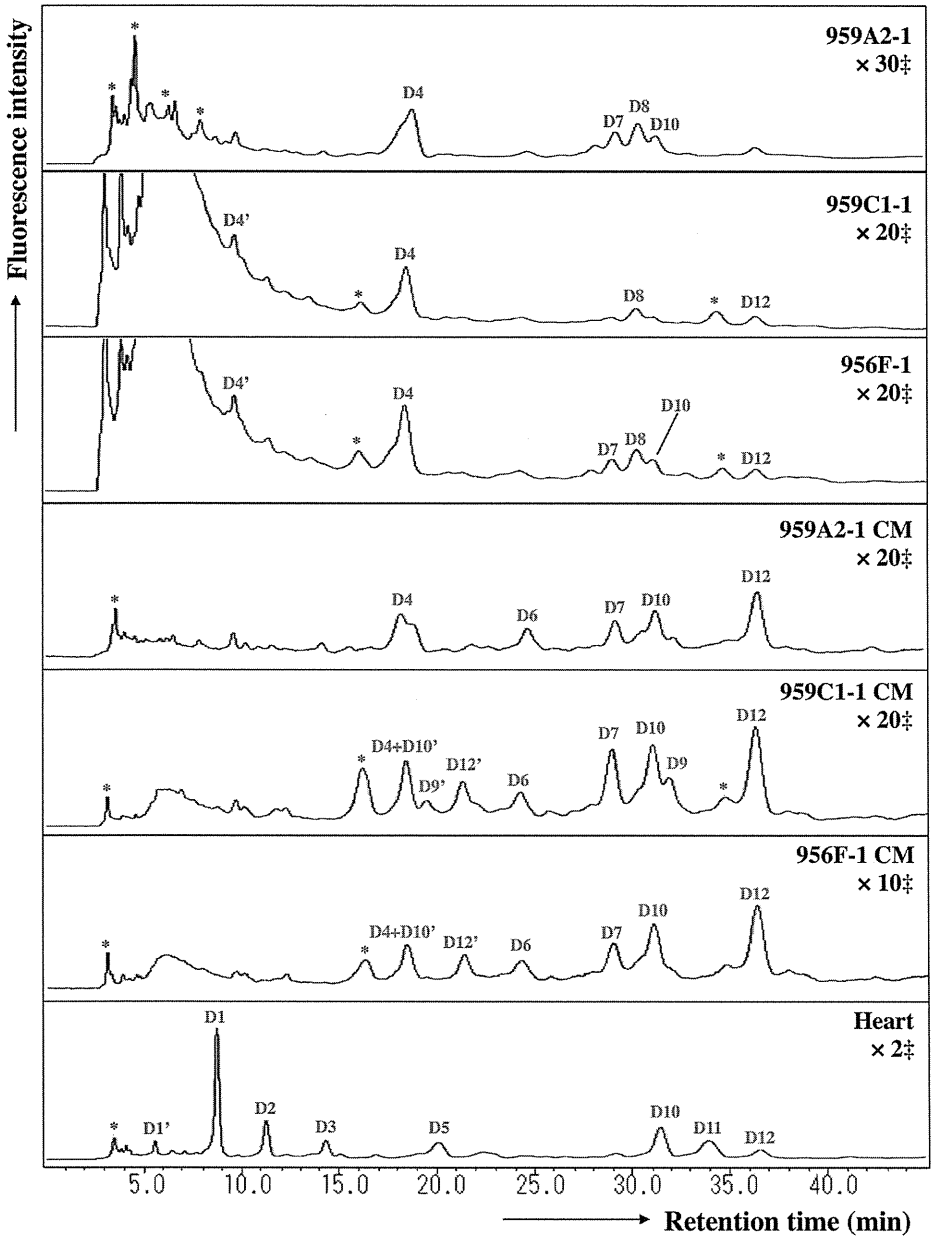

Figure 7. Reverse-phase ODS elution profiles of disialyl PA-glycans. The disialyl fractions were individually applied to the ODS column and eluted according to their hydrophobicity. D1′, D4′, D10′ and D12′: epimerization of D1, D4, D10 and D12; *Fractions containing no detectable PA-oligosaccharides. ‡Magnification ratio to the fluorescence intensity of asialoglycan of each sample.
doi:10.1371/journal.pone.0111064.g007

MS data. The coordinates of 54 *N*-glycans coincided with those for known references in the GALAXY database and their structures were identified. The coordinates for N9-3, M8, M11-2, M12, M13, M15, M17, M18, M19, M20-2, M21, M23, D8 and D9 did not correspond to known references.

N-glycans N9-2, M8, M12, M17, and M23 were trimmed by α-galactosidase but not by β-galactosidase or *N*-acetylglucosamidase. Their structures fit GALAXY references H5.12, 1A1-200.4, 1A3-200.4, 1A1-210.4, and 1A3-210.4, respectively. The galactosyl structures were then identified as Galα1-6Gal, because of the α-galactosidase-driven MS shifts. The structure of the M13 was identified by the coincidence with a GALAXY reference 1A2-H5.12 after being trimmed by α-L-fucosidase. The other *N*-glycans M11-2, M15, M18, M19, M20-2, M21, D8 and D9 were not identified in this study because they did not correspond to GALAXY references even after α-galactosidase digestions. They are described in Figure 8 and Table S1-S5 with their proposed formulas based on MALDI-TOF/MS data.

High-mannose *N*-Glycans were reduced by cardiomyogenic differentiation

The quantity of high-mannose *N*-glycans (HM) calculated from the total volume of N1–N6-2, N7 was highest in the iPSCs (959A2-1: 87.7%, 959C1-1: 68.3% and 956F-1: 78.2%), lower in the